AIAA JOURNAL
Vol. 41, No. 5, May 2003

Efficient Higher-Order Shell Theory for Laminated Composites with Multiple Delaminations

Jun-Sik Kim*
Inha University, Inchon 402-751, Republic of Korea
and
Maenghyo Cho†
Seoul National University, Seoul 151-742, Republic of Korea

A higher-order zigzag theory has been developed for laminated composite shells with multiple delaminations. General tensor-based formulation is developed for arbitrary curved shell with exact geometric description. A laminated shell theory with multiple delaminations for general lamination configurations is obtained by superposing a cubic varying displacement on a zigzag linearly varying displacement. The von Kármán nonlinearity is included in the formulation for the potentialities of addressing problems requiring geometric nonlinearity such as large deflection and postbuckling problems. When top and bottom surface transverse shear stress free conditions and interface transverse shear continuity conditions including delamination interfaces are imposed the displacement of the minimal degrees of freedom is obtained. The proposed displacement field can systematically handle the number, shape, size, and locations of the delaminations. Through the variational principle, equilibrium equations and variationally consistent boundary conditions are obtained. To assess the accuracy and efficiency of the present theory, the linear buckling problem of cylindrical shell with multiple delaminations has been analyzed. The higher-order zigzag theory should work as an efficient tool for analyzing the behavior of composite laminated shells with multiple delaminations.

I. Introduction

LAMINATED shell theories have received great attention in the past 30 years. For improved analysis of the behavior of composite shells, numerous studies have been reported. Extensive reviews can be found in the Refs. 1 and 2. For perfectly bonded laminated shells, three categories of higher-order shell theory have been developed. There are smeared,[3,4] layerwise,[5] and simplified zigzag theories.[6–8] Smeared theory is not adequate for detailed stress analysis because it cannot satisfy stress continuity conditions through the thickness of the laminates. Layerwise theory is sufficient to describe the deformation and stresses of the laminates through the thickness because it employs layer-dependent degrees of freedom. However, layerwise theory requires a large number of degrees of freedom for multilayered laminates. Thus, it is not efficient for engineering applications.

Because of its efficiency and accuracy, the simplified zigzag theory lately has received a great deal of attention. Within this model, displacement and stress continuity conditions and bounding surface stress free conditions are fulfilled. Moreover, it requires only five variables to describe the displacement field, and the variables do not depend on the number of layers.

Thus, from the computational point of view, zigzag theory has its own merits. Recently, zigzag higher-order theory has been extended to laminated plate and shell theories featuring imperfect interfaces.[9–11] However, these zigzag theories have not been applied to the problem involving delaminations with slipping and opening behaviors simultaneously. For the multiple delamination problem, an efficient higher-order zigzag theory has been developed for the plate problem[12] and now it is extended to shells with multiple delaminations. In the previous developments of zigzag higher-order theory with perfectly bonded layers, some geometrical assumptions were adopted. They are related to thinness assumption and doubly curved shallow shell assumptions. Recently, Gu and Chattopadhyay[13] developed a higher-order shell theory with delaminations under these assumptions. In the present study, a geometrically exact shell theory featuring multiple delaminations has been developed without limitations on the thickness ratio. The twisting curvature is also included in the shell model.

By the application of transverse shear stress continuity at the interfaces of the layers and zero shear traction conditions at the bounding surfaces, an efficient shell theory is derived to analyze the effect of multiple delaminations.

The theory involves only five primary variables in the undelaminated region, and it can systematically handle the number, size, shape, and location of delaminations. The present shell theory has minimal degrees of freedom to describe the deformation behavior of the multiply delaminated shell. Through the numerical study of the buckling of cylindrical shells with multiple delaminations, the efficiency and accuracy of the theory are demonstrated.

II. Preliminary Background

Composite shells with multiple delaminations are considered, consisting of a finite number N of orthotropic layers with uniform thickness h in a curvilinear coordinate system x^α. As shown in Fig. 1, the undeformed bottom surface $\Omega_{(0)}$ of the shell is chosen as the reference surface defined by $x^3 = 0$.

Let $\boldsymbol{r}$ be the position vector to a point on the bottom surface of the shell. In the shell theory, we are interested in the material points in a region of space near the reference surface. The position vector of any point of the three-dimensional space of the shell is written as

$$\boldsymbol{R}(x^\alpha, x^3) = \boldsymbol{r}(x^\alpha) + x^3 \boldsymbol{a}_3(x^\alpha) \tag{1}$$

where $\boldsymbol{a}_3$ is a unit vector perpendicular to the surface at point (x^α) and x^3 is the distance from the reference surface to the material point. The covariant base vector is defined as

$$\boldsymbol{g}_i = \frac{\partial \boldsymbol{R}}{\partial x^i} = \frac{\partial \boldsymbol{r}}{\partial x^i} + \frac{\partial}{\partial x^i}\left(x^3 \boldsymbol{a}_3\right) \tag{2}$$

Presented as Paper 2000-1400 at the AIAA Structures, Structural Dynamics, and Materials Conference, Atlanta, GA, 3–6 April 2000; received 12 February 2001; revision received 19 September 2001; accepted for publication 30 January 2002.

*Graduate Research Assistant, Department of Aerospace Engineering; currently Graduate Research Assistant, Department of Aerospace Engineering, Pennsylvania State University, University Park, PA 16802.

†Associate Professor, School of Mechanical and Aerospace Engineering; mhcho@snu.ac.kr.

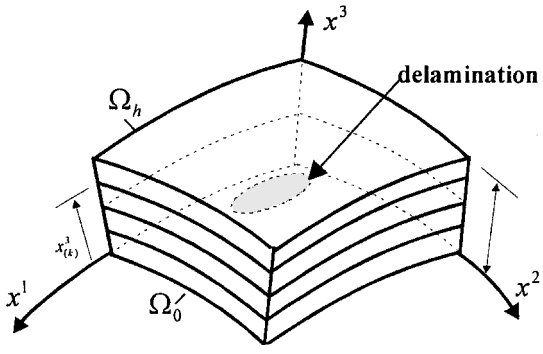

Fig. 1 Geometry of laminated shell with delaminations.

We will use the convention that Greek indices range over the value 1,2. Then

$$\boldsymbol{g}_\alpha = \boldsymbol{a}_\alpha + x^3 \boldsymbol{a}_{3,\alpha} \tag{3}$$

where $\boldsymbol{g}_3 = \boldsymbol{a}_3$ and $\boldsymbol{a}_\alpha = \boldsymbol{r}_{,\alpha}$ are vectors tangent to the surface coordinate curves and comma means partial differentiation.

We note that the vector $\mathrm{d}\boldsymbol{r}$ between two points an infinitesimal distance apart in the reference surface is

$$\mathrm{d}\boldsymbol{r} = \frac{\partial \boldsymbol{r}}{\partial x^\alpha}\,\mathrm{d}x^\alpha = \mathrm{d}x^\alpha \boldsymbol{a}_\alpha \tag{4}$$

The first fundamental form is defined by the metric tensor as follows:

$$\mathrm{d}s^2 = \mathrm{d}\boldsymbol{r}\cdot\mathrm{d}\boldsymbol{r} = a_{\alpha\beta}\,\mathrm{d}x^\alpha\,\mathrm{d}x^\beta \tag{5}$$

and surface tensor components $b_{\alpha\beta}$ is defined by the following linear mapping:

$$\boldsymbol{a}_{3,\alpha} = -b_{\alpha\beta}\boldsymbol{a}^\beta = -b^\beta_\alpha \boldsymbol{a}_\beta \tag{6}$$

where $\boldsymbol{a}^\alpha$ is the reciprocal base vectors to $\boldsymbol{a}_\alpha$. The second fundamental form is defined by the surface tensor as follows:

$$\mathrm{d}\boldsymbol{r}\cdot\mathrm{d}\boldsymbol{a}_3 = -b_{\alpha\beta}\,\mathrm{d}x^\alpha\,\mathrm{d}x^\beta = -b^\alpha_\beta\,\mathrm{d}x_\alpha\,\mathrm{d}x^\beta \tag{7}$$

where

$$b_{\alpha\beta} = -\boldsymbol{a}_\alpha\cdot\boldsymbol{a}_{3,\beta} = \boldsymbol{a}_3\cdot\boldsymbol{a}_{\alpha,\beta}, \qquad b^\alpha_\beta = b_{\beta\gamma}a^{\alpha\gamma} \tag{8}$$

Let the covariant base vectors $\boldsymbol{a}_i$ and $\boldsymbol{g}_i$ and contravariant base vectors $\boldsymbol{a}^i$ and $\boldsymbol{g}^i$ be introduced in the undeformed state of the shell as follows:

$$\boldsymbol{a}^3 = \boldsymbol{a}_3 = \frac{\boldsymbol{a}_1\times\boldsymbol{a}_2}{|\boldsymbol{a}_1\times\boldsymbol{a}_2|}, \qquad \boldsymbol{g}_\alpha = \mu^\beta_\alpha \boldsymbol{a}_\beta, \qquad \boldsymbol{g}^\beta = (\mu^{-1})^\beta_\alpha \boldsymbol{a}^\alpha \tag{9}$$

where μ^α_β and $(\mu^{-1})^\beta_\alpha$ denote the shifter tensor and its inverse, respectively. The shifter tensor and its inverse are expressed as follows:

$$\mu^\beta_\alpha = \delta^\beta_\alpha - x^3 b^\beta_\alpha, \qquad (\mu^{-1})^\beta_\alpha = (1/\mu)\epsilon^{\beta\lambda}\epsilon_{\alpha\nu}\mu^\nu_\lambda \tag{10}$$

where δ^β_α is the mixed Kronecker delta, $\epsilon^{\beta\lambda}$ and $\epsilon_{\alpha\nu}$ are the two-dimensional permutation tensors, and μ is the determinant of μ^β_α.

The displacement vector $\boldsymbol{V}(x^i)$ of the shell can be expressed as follows:

$$\boldsymbol{V} = V_\alpha\boldsymbol{g}^\alpha + V_3\boldsymbol{g}^3 = U_\alpha\boldsymbol{a}^\alpha + U_3\boldsymbol{a}^3, \qquad V_\alpha = \mu^\beta_\alpha U_\beta, \qquad V_3 = U_3 \tag{11}$$

The relationships between covariant differentiation of the three-dimensional components and two-dimensional components of the displacement vectors are expressed as

$$V_{\alpha|\beta} = \mu^\nu_\alpha(U_{\nu\|\beta} - b_{\nu\beta}U_3), \qquad V_{\alpha|3} = \mu^\beta_\alpha U_{\beta,3}$$
$$V_{3|\alpha} = U_{3\|\alpha} + b^\beta_\alpha U_\beta, \qquad V_{3|3} = U_{3\|3} \tag{12}$$

where $|$ and $\|$ denote the covariant derivatives in the three-dimensional space and two-dimensional space, respectively. These preliminary background is referred from Ref. 14 and also found in Refs. 15–18.

III. Displacement Model

To model the laminated composite shells with multiple delaminations, the representation of the displacement field is assumed as

$$U_\alpha(x^i) = u_\alpha + \psi_\alpha x^3 + \xi_\alpha(x^3)^2 + \phi_\alpha(x^3)^3 + \sum_{k=1}^{N-1} S^{(k)}_\alpha\left(x^3 - x^3_{(k)}\right)H\left(x^3 - x^3_{(k)}\right) + \sum_{k=1}^{N-1}\bar{u}^{(k)}_\alpha H\left(x^3 - x^3_{(k)}\right) \tag{13}$$

$$U_3(x^i) = u_3 + \sum_{k=1}^{N-1}\bar{u}^{(k)}_3 H\left(x^3 - x^3_{(k)}\right) \tag{14}$$

where u_i are the displacement of a point (x^α) on the reference surface, ψ_α are the rotations of the normal to the reference surface about the x^α coordinate, N is the number of layers, and $H(x^3 - x^3_{(k)})$ is the Heaviside unit step function. The variable $S^{(k)}_\alpha$ is the change of transverse shear angle in each layer. It is introduced to fulfill the continuity conditions of transverse shear stress at the perfectly bonded interfaces between the layers. The terms $\bar{u}^{(k)}_i$ represent possible jumps in the slipping and opening displacements, thus permitting incorporation of delamination for multilayered shells.

Green's strain tensor is expressed in the general curvilinear coordinate system:

$$e_{ij} = \tfrac{1}{2}\left(V_{i|j} + V_{j|i} + V^k_{|i}V_{k|j}\right) \tag{15}$$

Adopting the von Kármán partial nonlinearity, the strain components e_{ij} of the shell with initial imperfection of geometry can be obtained as the special case of Eq. (15) (Refs. 10, 17, and 18):

$$e_{\alpha\beta} = \tfrac{1}{2}\left(V_{\alpha|\beta} + V_{\beta|\alpha} + V_{3|\alpha}V_{3|\beta} + V_{3|\alpha}V^0_{3|\beta} + V^0_{3|\alpha}V_{3|\beta}\right)$$
$$e_{\alpha 3} = \tfrac{1}{2}(V_{\alpha|3} + V_{3|\alpha}), \qquad e_{33} = V_{3|3} \tag{16}$$

The covariant shear strain components of the shell with respect to $\boldsymbol{a}^i$ can be obtained as

$$2e_{\alpha 3} = U_{\alpha,3} + U_{3\|\alpha} + b^\beta_\alpha\left(U_\beta - x^3 U_{\beta,3}\right) \tag{17}$$

and the second kind Piola–Kirchhoff stress components of the shell can be obtained as follows from Refs. 7 and 15:

$$\sigma^{\alpha\beta} = H^{\alpha\beta\lambda\nu}e_{\lambda\nu}, \qquad \sigma^{\alpha 3} = 2E^{\alpha 3\lambda 3}e_{\lambda 3} \tag{18}$$

where E^{ijkl} are components of the elasticity tensor and $H^{\alpha\beta\lambda\nu} = E^{\alpha\beta\lambda\nu} - E^{\alpha\beta 33}E^{\lambda\nu 33}/E^{3333}$.

Substitution of Eqs. (13) and (14) into Eq. (16) yields the following transverse shear strain components in terms of the displacement components:

$$2e_{\alpha 3} = \psi_\alpha + u_{3\|\alpha} + b^\beta_\alpha u_\beta + \left\{2x^3\delta^\beta_\alpha - (x^3)^2 b^\beta_\alpha\right\}\xi_\beta + \left\{3(x^3)^2\delta^\beta_\alpha - 2(x^3)^3 b^\beta_\alpha\right\}\phi_\beta + \sum_{k=1}^{N-1}\left\{\left(\delta^\beta_\alpha - x^3_{(k)}b^\beta_\alpha\right)S^{(k)}_\beta + \bar{u}^{(k)}_{3\|\alpha} + b^\beta_\alpha\bar{u}^{(k)}_\beta\right\}H\left(x^3 - x^3_{(k)}\right) \tag{19}$$

$$= \psi_\alpha + u_{3\|\alpha} + b^\beta_\alpha u_\beta + 2(x^3)(\mu_1)^\beta_\alpha\xi_\beta + 3(x^3)^2(\mu_2)^\beta_\alpha\phi_\beta + \sum_{k=1}^{N-1}\left(\mu_{(k)}\right)^\beta_\alpha T^{(k)}_\beta H\left(x^3 - x^3_{(k)}\right) \tag{20}$$

where

$$(\mu_1)^\beta_\alpha = \left(\delta^\beta_\alpha - \tfrac{1}{2}x^3 b^\beta_\alpha\right), \qquad (\mu_2)^\beta_\alpha = \left(\delta^\beta_\alpha - \tfrac{2}{3}x^3 b^\beta_\alpha\right)$$
$$\left(\mu_{(k)}\right)^\beta_\alpha = \left(\delta^\beta_\alpha - x^3_{(k)}b^\beta_\alpha\right)$$
$$T^{(k)}_\beta = S^{(k)}_\beta + \left(\mu^{-1}_{(k)}\right)^\alpha_\beta\bar{u}^{(k)}_{3,\alpha} + \left(\mu^{-1}_{(k)}\right)^\alpha_\beta b^\gamma_\alpha\bar{u}^{(k)}_\gamma \tag{21}$$

The definition and the inverse of shifter tensor $(\mu^{-1}_{(k)})^\alpha_\beta$ for laminated shell in Eq. (21) was defined in Ref. 18. We assume initially that all

of the interfaces between the layers are delaminated. Then the number of delaminated layer interfaces is equal to the number of whole interfaces. The undelaminated interfaces can be easily simulated by setting $\bar{u}_i^{(k)}$ to be zero. Traction shear stress free conditions for the upper and lower surfaces of the shells require free strain conditions $e_{\alpha 3}|_{x^3=0,h}=0$ because the shear stresses depend only on the transverse shear strains for the orthotropic layer. Thus, the traction free condition can be written as

$$e_{\alpha 3}|_{x^3=0}=\psi_\alpha+u_{3\|\alpha}+b_\alpha^\beta u_\beta=0 \tag{22}$$

$$e_{\alpha 3}|_{x^3=h}=2h(\hat{\mu}_1)_\alpha^\beta\xi_\beta+3h^2(\hat{\mu}_2)_\alpha^\beta\phi_\beta+\sum_{k=1}^{N-1}\left(\mu_{(k)}\right)_\alpha^\beta T_\beta^{(k)}=0 \tag{23}$$

which are satisfied by

$$\psi_\alpha=-\left(u_{3\|\alpha}+b_\alpha^\beta u_\beta\right) \tag{24}$$

$$\xi_\beta=-\frac{\left(\hat{\mu}_1^{-1}\right)_\beta^\alpha}{2h}\left\{3h^2(\hat{\mu}_2)_\alpha^\gamma\phi_\gamma+\sum_{k=1}^{N-1}\left(\mu_{(k)}\right)_\alpha^\gamma T_\gamma^{(k)}\right\} \tag{25}$$

where

$$\begin{aligned}(\hat{\mu}_1)_\alpha^\beta&=(\mu_1)_\alpha^\beta\big|_{x^3=h}=\mu_\alpha^\beta\big|_{x^3=h/2}\\(\hat{\mu}_2)_\alpha^\beta&=(\mu_2)_\alpha^\beta\big|_{x^3=h}=\mu_\alpha^\beta\big|_{x^3=2h/3}\\\left(\hat{\mu}_1^{-1}\right)_\beta^\alpha&=(\mu^{-1})_\beta^\alpha\big|_{x^3=h/2}\end{aligned} \tag{26}$$

From Eqs. (24) and (25), the transverse shear strains are obtained by

$$2e_{\alpha 3}=d_\alpha^\gamma\phi_\gamma+\sum_{k=1}^{N-1}\left(\mu_{(k)}\right)_\lambda^\gamma T_\gamma^{(k)}\left\{\delta_\alpha^\lambda H\left(x^3-x_{(k)}^3\right)-c_\alpha^\lambda\frac{x^3}{h}\right\} \tag{27}$$

where

$$\begin{aligned}d_\alpha^\gamma&=3(x^3)^2(\mu_2)_\alpha^\gamma-3h(x^3)(\mu_1)_\alpha^\beta\left(\hat{\mu}_1^{-1}\right)_\beta^\lambda(\hat{\mu}_2)_\lambda^\gamma\\c_\alpha^\lambda&=(\mu_1)_\alpha^\beta\left(\hat{\mu}_1^{-1}\right)_\beta^\lambda\end{aligned} \tag{28}$$

At the perfectly bonded interfaces, transverse stresses should vary continuously. At the delaminated interfaces, transverse stresses are zero. In the present theory, at the delaminated interfaces, transverse shear stress continuity conditions are assumed to be satisfied because zero shear stresses also satisfy continuity of stresses. Thus in every interface, transverse shear stress continuity conditions are imposed. These continuity conditions can be written as

$${}^{(k)}\sigma^{\alpha 3}\big|_{x^3=x_{(k)}^3}={}^{(k+1)}\sigma^{\alpha 3}\big|_{x^3=x_{(k)}^3}\qquad(k=1,2,\ldots,N-1) \tag{29}$$

From the preceding equations and Eqs. (18) and (27), we obtain $2(N-1)$ linear algebraic equations of $2(N-1)$ unknowns $T_\gamma^{(k)}$. From this algebraic equation and Eq. (21), $T_\gamma^{(k)}$ and $S_\gamma^{(k)}$ can obtained as

$$T_\gamma^{(k)}=\left(a^{(k)}\right)_\gamma^\omega\phi_\omega \tag{30}$$

$$S_\gamma^{(k)}=\left(a^{(k)}\right)_\gamma^\omega\phi_\omega-\left\{\left(\mu_{(k)}^{-1}\right)_\gamma^\omega\bar{u}_{3,\omega}^{(k)}+\left(\mu_{(k)}^{-1}\right)_\gamma^\lambda b_\lambda^\omega\bar{u}_\omega^{(k)}\right\} \tag{31}$$

Thus continuity of transverse shear stresses between layers determines the change of slope $S_\alpha^{(k)}$ at each interface. In Eq. (31), the terms $(a^{(k)})_\gamma^\omega\phi_\omega$ represent the change in slope at each interface and depend only on the material properties of each layer. The terms $\bar{u}_{3,\omega}^{(k)}$ and $b_\lambda^\omega\bar{u}_\omega^{(k)}$ represent the change in slope of transverse deflection and in-surface stretching at each delamination interface, respectively.

Finally, substitution of Eqs. (24), (25), (30), and (31) into Eqs. (13) and (14) yields

$$U_\alpha=\mu_\alpha^\beta u_\beta-u_{3\|\alpha}x^3+f_\alpha^\beta\phi_\beta+\sum_{k=1}^{N-1}\left(g_{(k)}\right)_\alpha^\beta\bar{u}_{3\|\beta}^{(k)}+\sum_{k=1}^{N-1}\left(h_{(k)}\right)_\alpha^\beta\bar{u}_\beta^{(k)} \tag{32}$$

$$U_3=u_3+\sum_{k=1}^{N-1}\bar{u}_3^{(k)}H\left(x^3-x_{(k)}^3\right) \tag{33}$$

where

$$\begin{aligned}f_\alpha^\beta&=\delta_\alpha^\beta(x^3)^3-\frac{3h}{2}(x^3)^2\left(\hat{\mu}_1^{-1}\right)_\alpha^\gamma(\hat{\mu}_2)_\gamma^\beta\\&\quad-\frac{1}{2h}(x^3)^2\left(\hat{\mu}_1^{-1}\right)_\alpha^\lambda\sum_{k=1}^{N-1}\left(\mu_{(k)}\right)_\lambda^\gamma\left(a^{(k)}\right)_\gamma^\beta\\&\quad+\sum_{k=1}^{N-1}\left(a^{(k)}\right)_\alpha^\beta\left(x^3-x_{(k)}^3\right)H\left(x^3-x_{(k)}^3\right)\end{aligned} \tag{34}$$

$$\left(g_{(k)}\right)_\alpha^\beta=-\left(\mu_{(k)}^{-1}\right)_\alpha^\beta\left(x^3-x_{(k)}^3\right)H\left(x^3-x_{(k)}^3\right) \tag{35}$$

$$\left(h_{(k)}\right)_\alpha^\beta=\left\{\delta_\alpha^\beta-\left(\mu_{(k)}^{-1}\right)_\alpha^\lambda b_\lambda^\beta\left(x^3-x_{(k)}^3\right)\right\}H\left(x^3-x_{(k)}^3\right) \tag{36}$$

If in Eqs. (32) and (33) the terms $\bar{u}_i^{(k)}$ are neglected, the considered displacement field is similar to that postulated by He.[7] If we neglect the curvature terms, then this field reduces to the plate version given by Cho and Kim.[12]

Recently, laminated composite plates and shells with interlaminar bonding imperfections have been developed. Slipping interface conditions were provided by Cheng et al.,[9] Cheng and Kitipornchai,[10] Di Sciuva,[11] and Schmidt and Librescu.[18] Slipping as well as normal displacement jumps are considered by Librescu and Schmidt.[19] Most of the theories adopt a spring-layer model, which is given as

$$\bar{u}_\alpha^{(k)}=R_{\alpha\beta}^{(k)}(x^\rho)\sigma^{\beta 3}\left(x^\rho,x_{(k)}^3\right),\qquad\bar{u}_3^{(k)}=R_{33}^{(k)}(x^\rho)\sigma^{33}\left(x^\rho,x_{(k)}^3\right) \tag{37}$$

For case 1, if $R_{\alpha\beta}$, $R_{33}\to 0$, there is no jump between layers. This condition indicates the perfectly bonded interface case.

For case 2, if $R_{\alpha\beta}$, $R_{33}\to\infty$, it represents the completely debonded case.

For case 3, if $R_{\alpha\beta}\to\infty$, and $R_{33}\to 0$, it represents the perfect slipping condition without friction, that is, perfectly lubricated interfaces.

In the present study, we consider case 2, which is the completely debonded case in the delaminated zone.

IV. Equilibrium Equation and Boundary Conditions

The equations of equilibrium and the variationally consistent boundary conditions are formulated in a weak form via the principle of virtual work. The principle of virtual work without body forces is given by

$$\int_v\left(\sigma^{\alpha\beta}\delta e_{\alpha\beta}+2\sigma^{\alpha 3}\delta e_{\alpha 3}\right)\mathrm{d}v-\int_A s^i\delta V_i\,\mathrm{d}A-\int_\Omega p^i\delta V_i\,\mathrm{d}\Omega=0 \tag{38}$$

where s^i are the prescribed components of the stress vector per unit area of lateral surface A of the shell, v is the volume of the shell, and p^i are the prescribed components of stress vector per unit area of the surfaces Ω_0 and Ω_h.

The equations of equilibrium of the present theory can be derived by integrating the derivatives of the varied quantities by parts and collecting the coefficients of δu_α, δu_3, $\delta\phi_\alpha$, $\delta\bar{u}_\alpha^{(k)}$, and $\delta\bar{u}_3^{(k)}$:

$$\delta u_\alpha:N^{(1)\alpha}+R^{(2)\alpha}-M_{\|\beta}^{(1)\alpha\beta}=0$$

$$\delta u_3:N^{(1)3}+R_{\|\alpha}^{(1)\alpha}+M_{\|\alpha\beta}^{(2)\alpha\beta}+p^3=0$$

$$\delta\phi_\alpha : N^{(2)\alpha} + N^{(3)\alpha} + R^{(3)\alpha} - M^{(3)\alpha\beta}_{\|\beta} = 0$$

$$\delta\bar{u}^{(k)}_\alpha : \bar{N}^{(2)\alpha}_{(k)} + \bar{R}^{(3)\alpha}_{(k)} - \bar{M}^{(2)\alpha\beta}_{(k)\|\beta} = 0$$

$$\delta\bar{u}^{(k)}_3 : \bar{N}^{(1)}_{(k)} + \left(\bar{N}^{(1)\alpha}_{(k)} + \bar{R}^{(1)\alpha}_{(k)} + \bar{R}^{(2)\alpha}_{(k)}\right)_{\|\alpha} + \bar{M}^{(1)\alpha\beta}_{(k)\|\alpha\beta} = 0 \quad (39)$$

and the associated boundary conditions are specified as

$$\delta u_n = 0 \quad \text{or} \quad M^{(1)\alpha\beta} n_\alpha n_\beta = S^{(1)\alpha} n_\alpha$$

$$\delta u_t = 0 \quad \text{or} \quad M^{(1)\alpha\beta} t_\alpha n_\beta = S^{(1)\alpha} t_\alpha$$

$$\delta u_3 = 0 \quad \text{or} \quad \left(R^{(1)\beta} + M^{(2)\alpha\beta}{}_{\|\alpha}\right) n_\beta + \frac{\partial}{\partial t}\left(M^{(2)\alpha\beta} t_\alpha n_\beta\right) = S^{(1)3} + \frac{\partial}{\partial t}\left(S^{(2)\alpha} t_\alpha\right)$$

$$\delta\phi_n = 0 \quad \text{or} \quad M^{(3)\alpha\beta} n_\alpha n_\beta = S^{(3)\alpha} n_\alpha$$

$$\delta\phi_t = 0 \quad \text{or} \quad M^{(3)\alpha\beta} t_\alpha n_\beta = S^{(3)\alpha} t_\alpha$$

$$\delta\left(\frac{\partial u_3}{\partial n}\right) = 0 \quad \text{or} \quad M^{(2)\alpha\beta} n_\alpha n_\beta = S^{(2)\alpha} n_\alpha$$

$$\delta\bar{u}^{(k)}_n = 0 \quad \text{or} \quad \bar{M}^{(2)\alpha\beta}_{(k)} n_\alpha n_\beta = \bar{S}^{(2)\alpha}_{(k)} n_\alpha$$

$$\delta\bar{u}^{(k)}_t = 0 \quad \text{or} \quad \bar{M}^{(2)\alpha\beta}_{(k)} t_\alpha n_\beta = \bar{S}^{(2)\alpha}_{(k)} t_\alpha$$

$$\delta\bar{u}^{(k)}_3 = 0 \quad \text{or} \quad \left(\bar{N}^{(1)\beta}_{(k)} + \bar{R}^{(1)\beta}_{(k)} + \bar{R}^{(2)\beta}_{(k)} - \bar{M}^{\alpha\beta}_{(k)\|\alpha}\right) n_\beta + \frac{\partial}{\partial t}\left(\bar{M}^{(1)\alpha\beta}_{(k)} t_\alpha n_\beta\right) = \bar{S}^{(1)3}_{(k)} + \frac{\partial}{\partial t}\left(\bar{S}^{(1)\alpha}_{(k)} t_\alpha\right)$$

$$\delta\left(\frac{\bar{u}^{(k)}_3}{\partial n}\right) = 0 \quad \text{or} \quad \bar{M}^{(1)\alpha\beta}_{(k)} n_\alpha n_\beta = \bar{S}^{(1)\alpha}_{(k)} n_\alpha \quad (40)$$

in which

$$\left[N^{(1)\alpha}, N^{(2)\alpha}, N^{(1)3}\right] = \int_0^h \sigma^{\gamma\beta}\mu^\lambda_\gamma\left[\mu^\alpha_{\lambda\|\beta}, f^\alpha_{\lambda\|\beta}, b_{\lambda\beta}\right]\mu\,\mathrm{d}x^3$$

$$N^{(3)\alpha} = \int_0^h \sigma^{\gamma 3}\left(\mu^\lambda_\gamma f^\alpha_{\lambda,3} + b^\lambda_\gamma f^\alpha_\lambda\right)\mu\,\mathrm{d}x^3$$

$$\left[\bar{N}^{(1)\alpha}_{(k)}, \bar{N}^{(2)\alpha}_{(k)}, \bar{N}^{(1)3}_{(k)}\right] = \int_0^h \sigma^{\gamma\beta}\mu^\lambda_\gamma\left[\left(g_{(k)}\right)^\alpha_{\lambda\|\beta}, \left(h_{(k)}\right)^\alpha_{\lambda\|\beta}, b_{\lambda\beta}H\left(x^3 - x^3_{(k)}\right)\right]\mu\,\mathrm{d}x^3$$

$$\left[M^{(1)\alpha\beta}, M^{(2)\alpha\beta}, M^{(3)\alpha\beta}\right] = \int_0^h \sigma^{\gamma\beta}\mu^\lambda_\gamma\left[\mu^\alpha_\lambda, x^3\delta^\alpha_\lambda, f^\alpha_\lambda\right]\mu\,\mathrm{d}x^3$$

$$\left[\bar{M}^{(1)\alpha\beta}_{(k)}, \bar{M}^{(2)\alpha\beta}_{(k)}\right] = \int_0^h \sigma^{\gamma\beta}\mu^\lambda_\gamma\left[\left(g_{(k)}\right)^\alpha_\lambda, \left(h_{(k)}\right)^\alpha_\lambda\right]\mu\,\mathrm{d}x^3$$

$$\left[R^{(1)\alpha}, R^{(2)\alpha}, R^{(3)\alpha}\right] = \int_0^h \sigma^{\gamma\beta}\left(V_{3|\gamma} + V^0_{3|\gamma}\right)\left[\mu^\alpha_\beta,\ b^\lambda_\beta\mu^\alpha_\lambda, b^\lambda_\beta f^\alpha_\lambda\right]\mu\,\mathrm{d}x^3$$

$$\left[\bar{R}^{(1)\alpha}_{(k)}, \bar{R}^{(2)\alpha}_{(k)}, \bar{R}^{(3)\alpha}_{(k)}\right] = \int_0^h \sigma^{\gamma\beta}\left(V_{3|\gamma} + V^0_{3|\gamma}\right) \times \left[\delta^\alpha_\beta H\left(x^3 - x^3_{(k)}\right), \left(g_{(k)}\right)^\alpha_\beta, \left(h_{(k)}\right)^\alpha_\beta\right]\mu\,\mathrm{d}x^3$$

$$\left[S^{(1)\alpha}, S^{(2)\alpha}, S^{(3)\alpha}\right] = \int_0^h s^{\gamma\beta}\left[\mu^\alpha_\gamma, x^3\delta^\alpha_\gamma, f^\alpha_\gamma\right]n_\beta\mu\,\mathrm{d}x^3$$

$$S^{(1)3} = \int_0^h s^{3\beta} n_\beta\mu\,\mathrm{d}x^3, \qquad \bar{S}^{(1)3}_{(k)} = \int_0^h s^{3\beta} H\left(x^3 - x^3_{(k)}\right)n_\beta\mu\,\mathrm{d}x^3$$

$$\left[\bar{S}^{(1)\alpha}_{(k)}, \bar{S}^{(2)\alpha}_{(k)}\right] = \int_0^h s^{\gamma\beta}\left[\left(g_{(k)}\right)^\alpha_\gamma, \left(h_{(k)}\right)^\alpha_\gamma\right]n_\beta\mu\,\mathrm{d}x^3$$

where $p^3 = \mu|_{x^3=h}\, p^3_h + p^3_0$, and s^{ij} are components of s^i with respect to $\boldsymbol{g}_j$.

V. Shallow Shell Theory Counterpart

For shallow shells, an appropriate simplification $\mu^\beta_\alpha \to \delta^\beta_\alpha$ can be considered. As a result,

$$g_{\alpha\beta} = a_{\alpha\beta}, \qquad g^{\alpha\beta} = a^{\alpha\beta}, \qquad \mu \to 1 \quad (41)$$

When this assumption is applied to Eq. (32), the displacement field is obtained as follows:

$$U_\alpha = \left(\delta^\beta_\alpha - \underline{b^\beta_\alpha x^3}\right)u_\beta - u_{3,\alpha}x^3 - \Lambda^\beta_a\phi_\beta(x^3)^2 + \phi_\alpha(x^3)^3 + \sum_{k=1}^{N-1}\left[\left\{\left(a^{(k)}\right)^\beta_\alpha\phi_\beta - \bar{u}^{(k)}_{3,\alpha}\right\}\left(x^3 - x^3_{(k)}\right) + \bar{u}^{(k)}_\beta\left\{\delta^\beta_\alpha - \underline{b^\beta_\alpha\left(x^3 - x^3_{(k)}\right)}\right\}\right]H\left(x^3 - x^3_{(k)}\right) \quad (42)$$

$$U_3 = u_3 + \sum_{k=1}^{N-1}\bar{u}^{(k)}_3 H\left(x^3 - x^3_{(k)}\right) \quad (43)$$

where

$$\Lambda^\beta_\alpha = \frac{3h}{2}\delta^\beta_\alpha + \frac{1}{2h}\sum_{k=1}^{N-1}\left(a^{(k)}\right)^\beta_\alpha \quad (44)$$

In Eq. (41), the underlined terms in the expressions of in-surface displacement fields do not provide any significant effect when dealing with shallow shell theory. They are the order of (h/R). The reason for keeping these terms is that a simple expression for the transverse shear strains can be obtained whose form is almost the same with that corresponding to plate theory.[12]

From Eq. (16), the strain components associated with the small-displacement theory for shallow shells are obtained as

$$e_{\alpha\beta} = \tfrac{1}{2}(U_{\alpha,\beta} + U_{\beta,\alpha}) - \bar{\Gamma}^\nu_{\alpha\beta}U_\nu - b_{\alpha\beta}U_3 \quad (45)$$

$$e_{\alpha 3} = \tfrac{1}{2}\left(U_{\alpha,3} + U_{3,\alpha} + b^\beta_\alpha U_\beta\right) \quad (46)$$

where $\bar{\Gamma}^\nu_{\alpha\beta}$ is the second kind of Christoffel symbol for two-dimensional shell space. The strain components are defined by collecting the terms involving the coefficients of the same power of x^3 power terms and Heaviside unit step function:

$$e_{\alpha\beta} = e^{(0)}_{\alpha\beta} + e^{(1)}_{\alpha\beta}x^3 + e^{(2)}_{\alpha\beta}(x^3)^2 + e^{(3)}_{\alpha\beta}(x^3)^3 + \sum_{k=1}^{(N-1)}e^k_{\alpha\beta}\left(x^3 - x^3_{(k)}\right)H\left(x^3 - x^3_{(k)}\right) + \sum_{k=1}^{(N-1)}\bar{e}^k_{\alpha\beta}H\left(x^3 - x^3_{(k)}\right)$$

$$e_{\alpha 3} = e^{(1)}_{\alpha 3}x^3 + e^{(2)}_{\alpha 3}(x^3)^2 + \sum_{k=1}^{(N-1)}e^{(k)}_{\alpha 3}H\left(x^3 - x^3_{(k)}\right) \quad (47)$$

where

$$e^{(0)}_{\alpha\beta} = \tfrac{1}{2}(u_{\alpha,\beta} + u_{\beta,\alpha}) - \bar{\Gamma}^\nu_{\alpha\beta}u_\nu - b_{\alpha\beta}u_3$$

$$\epsilon^{(1)}_{\alpha\beta} = -\tfrac{1}{2}\left(b^\omega_{\alpha,\beta}u_\omega + b^\gamma_{\beta,\alpha}u_\gamma + b^\omega_\alpha u_{\omega,\beta} + b^\gamma_\beta u_{\gamma,\alpha}\right) - u_{3,\alpha\beta} + \bar{\Gamma}^\nu_{\alpha\beta}\left(b^\lambda_\nu u_\lambda + u_{3,\nu}\right)$$

$$e^{(2)}_{\alpha\beta} = -\tfrac{1}{2}\left(\Lambda^\gamma_\alpha\phi_{\gamma,\beta} + \Lambda^\lambda_\beta\phi_{\lambda,\alpha}\right) + \bar{\Gamma}^\nu_{\alpha\beta}\Lambda^\omega_\nu\phi_\omega$$

$$e^{(3)}_{\alpha\beta} = \tfrac{1}{2}(\phi_{\alpha,\beta} + \phi_{\beta,\alpha}) - \bar{\Gamma}^\nu_{\alpha\beta}\phi_\nu$$

$$e^k_{\alpha\beta} = \tfrac{1}{2}\left\{\left(a^{(k)}\right)^\gamma_\alpha\phi_{\gamma\beta} + \left(a^{(k)}\right)^\omega_\beta\phi_{\omega,\alpha}\right\} - \bar{u}^{(k)}_{3,\alpha\beta} - \tfrac{1}{2}\left(b^\omega_{\alpha,\beta}\bar{u}^{(k)}_\omega + b^\gamma_{\beta,\alpha}\bar{u}^{(k)}_\gamma + b^\omega_\alpha\bar{u}^{(k)}_{\omega,\beta} + b^\gamma_\beta\bar{u}^{(k)}_{\gamma,\alpha}\right) - \bar{\Gamma}^\nu_{\alpha\beta}\left\{\left(a^{(k)}\right)^\lambda_\nu\phi_\lambda - \bar{u}^{(k)}_{3,\nu} - b^\lambda_\nu\bar{u}^{(k)}_\lambda\right\}$$

$$\bar{e}^k_{\alpha\beta} = \tfrac{1}{2}\left(\bar{u}^{(k)}_{\alpha,\beta} + \bar{u}^{(k)}_{\beta,\alpha}\right) - \bar{\Gamma}^{v}_{\alpha\beta}\bar{u}^{(k)}_{v} - b_{\alpha\beta}\bar{u}^{(k)}_{3}$$

$$2e^{(1)}_{\alpha 3} = -2\Lambda^{\gamma}_{\alpha}\phi_{\gamma}, \qquad 2e^{(2)}_{\alpha 3} = 3\phi_{\alpha}, \qquad 2e^{k}_{\alpha 3} = \left(a^{(k)}\right)^{\gamma}_{\alpha}\phi_{\gamma} \tag{48}$$

The virtual work principle for bifurcation buckling analysis is given by

$$\int_v \left(\sigma^{\alpha\beta}\delta e_{\alpha\beta} + 2\sigma^{\alpha 3}\delta e_{\alpha 3}\right) \mathrm{d}v - \int_A N^{(0)\alpha\beta} U_{3,\alpha}\delta U_{3,\beta}\, \mathrm{d}A = 0 \tag{49}$$

where $N^{(0)\alpha\beta}$ are the constant in-surface edge loads.

To derive the explicit constitutive equations for shallow shells, the stresses resultants are redefined. The detailed procedure is omitted for the sake of simplicity; see Ref. 12. Thus, the constitutive equations of the laminated shallow shells are given by

$$\begin{Bmatrix} N^{\alpha\beta} \\ M^{\alpha\beta} \\ R^{(2)\alpha\beta} \\ R^{(3)\alpha\beta} \\ {}^{i}\bar{M}^{\alpha\beta} \\ {}^{i}\bar{N}^{\alpha\beta} \end{Bmatrix} = \begin{bmatrix} A^{(0)\alpha\beta\gamma\omega} & A^{(1)\alpha\beta\gamma\omega} & A^{(2)\alpha\beta\gamma\omega} & A^{(3)\alpha\beta\gamma\omega} & {}^{j}B^{(0)\alpha\beta\gamma\omega} & {}^{j}E^{(0)\alpha\beta\gamma\omega} \\ A^{(1)\alpha\beta\gamma\omega} & A^{(2)\alpha\beta\gamma\omega} & A^{(3)\alpha\beta\gamma\omega} & A^{(4)\alpha\beta\gamma\omega} & {}^{j}B^{(1)\alpha\beta\gamma\omega} & {}^{j}E^{(1)\alpha\beta\gamma\omega} \\ A^{(2)\alpha\beta\gamma\omega} & A^{(3)\alpha\beta\gamma\omega} & A^{(4)\alpha\beta\gamma\omega} & A^{(5)\alpha\beta\gamma\omega} & {}^{j}B^{(2)\alpha\beta\gamma\omega} & {}^{j}E^{(2)\alpha\beta\gamma\omega} \\ A^{(3)\alpha\beta\gamma\omega} & A^{(4)\alpha\beta\gamma\omega} & A^{(5)\alpha\beta\gamma\omega} & A^{(6)\alpha\beta\gamma\omega} & {}^{j}B^{(3)\alpha\beta\gamma\omega} & {}^{j}E^{(3)\alpha\beta\gamma\omega} \\ {}^{i}B^{(0)\alpha\beta\gamma\omega} & {}^{i}B^{(1)\alpha\beta\gamma\omega} & {}^{i}B^{(2)\alpha\beta\gamma\omega} & {}^{i}B^{(3)\alpha\beta\gamma\omega} & {}^{ij}D^{\alpha\beta\gamma\omega} & {}^{ij}F^{\alpha\beta\gamma\omega} \\ {}^{i}E^{(0)\alpha\beta\gamma\omega} & {}^{i}E^{(1)\alpha\beta\gamma\omega} & {}^{i}E^{(2)\alpha\beta\gamma\omega} & {}^{i}E^{(3)\alpha\beta\gamma\omega} & {}^{ij}F^{\alpha\beta\gamma\omega} & {}^{ij}E^{\alpha\beta\gamma\omega} \end{bmatrix} \begin{Bmatrix} e^{(0)}_{\gamma\omega} \\ e^{(1)}_{\gamma\omega} \\ e^{(2)}_{\gamma\omega} \\ e^{(3)}_{\gamma\omega} \\ e^{j}_{\gamma\omega} \\ \bar{e}^{j}_{\gamma\omega} \end{Bmatrix} \tag{50}$$

$$\begin{Bmatrix} V^{(1)\alpha} \\ V^{(2)\alpha} \\ {}^{i}Q^{\alpha} \end{Bmatrix} = \begin{bmatrix} A^{(2)\alpha 3\beta 3} & A^{(3)\alpha 3\beta 3} & {}^{j}E^{(1)\alpha 3\beta 3} \\ A^{(3)\alpha 3\beta 3} & A^{(4)\alpha 3\beta 3} & {}^{j}E^{(2)\alpha 3\beta 3} \\ {}^{i}E^{(1)\alpha 3\beta 3} & {}^{i}E^{(2)\alpha 3\beta 3} & {}^{ij}E^{\alpha 3\beta 3} \end{bmatrix} \begin{Bmatrix} 2e^{(1)}_{\beta 3} \\ 2e^{(2)}_{\beta 3} \\ 2e^{j}_{\beta 3} \end{Bmatrix} \tag{51}$$

where

$$A^{(m)\alpha\beta\gamma\omega} = \sum_{k=1}^{N}\int_{x^3_k}^{x^3_{k+1}} \bar{Q}^{(k)\alpha\beta\gamma\omega}(x^3)^m\, \mathrm{d}x^3 \qquad (m = 0, 1, 2, 3, 4, 5, 6)$$

$${}^{j}B^{(m)\alpha\beta\gamma\omega} = \sum_{k=1}^{N}\int_{x^3_k}^{x^3_{k+1}} \bar{Q}^{(k)\alpha\beta\gamma\omega}\left(x^3 - x^3_{(j)}\right)H\left(x^3 - x^3_{(j)}\right)(x^3)^m\, \mathrm{d}x^3 \qquad (m = 0, 1, 2, 3)$$

$${}^{j}E^{(m)\alpha\beta\gamma\omega} = \sum_{k=1}^{N}\int_{x^3_k}^{x^3_{k+1}} \bar{Q}^{(k)\alpha\beta\gamma\omega}H\left(x^3 - x^3_{(j)}\right)(x^3)^m\, \mathrm{d}x^3 \qquad (m = 0, 1, 2, 3)$$

$${}^{ij}E^{\alpha\beta\gamma\omega} = \sum_{k=1}^{N}\int_{x^3_k}^{x^3_{k+1}} \bar{Q}^{(k)\alpha\beta\gamma\omega}H\left(x^3 - x^3_{(i)}\right)H\left(x^3 - x^3_{(j)}\right)\mathrm{d}x^3$$

$${}^{ij}F^{\alpha\beta\gamma\omega} = \sum_{k=1}^{N}\int_{x^3_k}^{x^3_{k+1}} \bar{Q}^{(k)\alpha\beta\gamma\omega}\left(x^3 - x^3_{(i)}\right) \times H\left(x^3 - x^3_{(i)}\right)H\left(x^3 - x^3_{(j)}\right)\mathrm{d}x^3$$

$${}^{ij}D^{\alpha\beta\gamma\omega} = \sum_{k=1}^{N}\int_{x^3_k}^{x^3_{k+1}} \bar{Q}^{(k)\alpha\beta\gamma\omega}\left(x^3 - x^3_{(i)}\right)\left(x^3 - x^3_{(j)}\right) \times H\left(x^3 - x^3_{(i)}\right)H\left(x^3 - x^3_{(j)}\right)\mathrm{d}x^3$$

$$A^{(m)\alpha 3\gamma 3} = \sum_{k=1}^{N}\int_{x^3_k}^{x^3_{k+1}} \bar{Q}^{(k)\alpha 3\gamma 3}(x^3)^m\, \mathrm{d}x^3 \qquad (m = 2, 3, 4)$$

$${}^{j}E^{(m)\alpha 3\gamma 3} = \sum_{k=1}^{N}\int_{x^3_k}^{x^3_{k+1}} \bar{Q}^{(k)\alpha 3\gamma 3}H\left(x^3 - x^3_{(j)}\right)(x^3)^m\, \mathrm{d}x^3 \qquad (m = 1, 2)$$

$${}^{ij}E^{\alpha 3\gamma 3} = \sum_{k=1}^{N}\int_{x^3_k}^{x^3_{k+1}} \bar{Q}^{(k)\alpha 3\gamma 3}H\left(x^3 - x^3_{(i)}\right)H\left(x^3 - x^3_{(j)}\right)\mathrm{d}x^3$$

where $\bar{Q}^{(k)\alpha\beta\gamma\omega}$ are the modified reduced material moduli for each lamina. The equilibrium equations and boundary conditions of shallow shell version are omitted here because of limited space.

VI. Finite Element Model

To examine the accuracy of the present shallow shell theory, bifurcation buckling problems for laminated composite cylindrical shell with multiple delaminations are considered (Fig. 2). For cylindrical shells, the in-surface metric tensor, Christoffel symbol, and curvature tensor are found:

$$[a_{\alpha\beta}] = \begin{bmatrix} 1 & 0 \\ 0 & 1 \end{bmatrix}, \qquad \bar{\Gamma}^{v}_{\alpha\beta} = 0, \qquad [b_{\alpha\beta}] = \left[b^{\alpha}_{\beta}\right] = \begin{bmatrix} 0 & 0 \\ 0 & -1/R \end{bmatrix} \tag{52}$$

A semi-analytical method is used to solve the system equations. Finite element discretization is performed for the axial direction, and analytical harmonic expansions are used for the circumferential direction. In this work, the finite element displacements u_α, u_3, ϕ_α, $\bar{u}^k_\alpha$, and $\bar{u}^k_3$ are expressed in the following form:

$$\left[u_1, \phi_1, \bar{u}^k_1\right] = \sum_{m=1}^{M}\psi_m(x^1)\left[u^{mn}_1, \phi^{mn}_1, \bar{u}^{(k)mn}_1\right]\cos\left(n\frac{x^2}{R}\right) \tag{53}$$

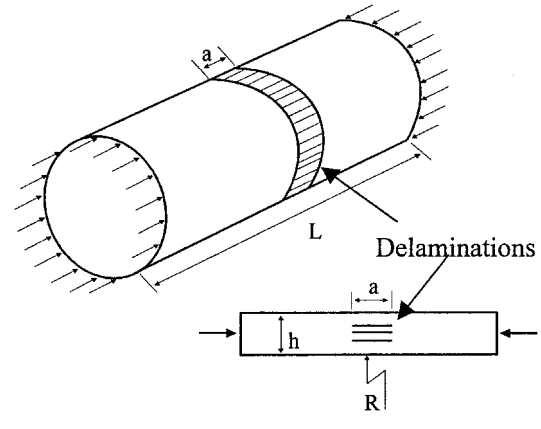

Fig. 2 Geometry and loading of cylindrical shells with multiple delaminations.

$$\left[u_2, \phi_2, \bar{u}_2^k\right] = \sum_{m=1}^{M} \psi_m(x^1)\left[u_2^{mn}, \phi_2^{mn}, \bar{u}_2^{(k)mn}\right] \sin\left(n\frac{x^2}{R}\right) \quad (54)$$

$$u_3 = \sum_{m=1}^{M} \left[P_m(x^1)u_3^{mn} + H_m(x^1)u_{3,1}^{mn}\right] \cos\left(n\frac{x^2}{R}\right) \quad (55)$$

$$\bar{u}_3^k = \sum_{m=1}^{M} \left[P_m(x^1)\bar{u}_3^{(k)mn} + H_m(x^1)\bar{u}_{3,1}^{(k)mn}\right] \cos\left(n\frac{x^2}{R}\right) \quad (56)$$

where M is the number of nodes in a typical finite element and n (only one due to the orthogonality of sin $n\theta$ and cos $n\theta$) is the circumferential wave number. Here, ψ_m is a linear Lagrangian interpolation function, and P_m and H_m are Hermite cubic interpolation functions.

Substituting Eqs. (52–55) into Eq.(48), we obtain the following eigenvalue problem:

$$([\boldsymbol{K}] - \lambda[\boldsymbol{S}])\{\boldsymbol{u}\} = \{\boldsymbol{0}\} \quad (57)$$

where $[\boldsymbol{K}]$ and $[\boldsymbol{G}]$ are the stiffness matrix and the geometric stiffness matrix, respectively. In the present bifurcation buckling analysis, it is assumed that there is no contact between the delaminated interfaces. For a given configuration, the circumferential wave number is varied to determine the lowest buckling load.

VII. Numerical Examples

In this study, the symmetric and antisymmetric modes are investigated using a half model of the laminated cylindrical shell. The typical finite element model is shown in Fig. 3. The following clamped boundary conditions for symmetric and antisymmetric modes are assumed:

At $x = 0, L$,

$$u_\alpha = 0, \qquad u_3 = 0, \qquad u_{3,1} = 0, \qquad \phi_\alpha = 0$$
$$\bar{u}_\alpha^k = 0, \qquad \bar{u}_3^k = 0, \qquad \bar{u}_{3,1}^k = 0 \quad (58)$$

At $x = L/2$ for symmetric mode,

$$u_1 = 0, \qquad u_{3,1} = 0, \qquad \phi_1 = 0, \qquad \bar{u}_1^k = 0, \qquad \bar{u}_{3,1}^k = 0 \quad (59)$$

At $x = L/2$ for antisymmetric mode,

$$u_2 = 0, \qquad u_3 = 0, \qquad \phi_2 = 0, \qquad \bar{u}_2^k = 0, \qquad \bar{u}_3^k = 0 \quad (60)$$

A. Isotropic Shell

To examine the accuracy of the present theory, a clamped isotropic shell is considered. The dimensions of the shell are such that $L/\hat{R} = 5$ and $\hat{R}/h = 30$, where L is the axial length of the shell and $\hat{R}$ is $R + h/2$. The numerical results of the variation of critical load with delamination length, obtained using the present theory, are compared with those obtained using existing solutions. Normalized buckling loads of a laminated shell with a single delamination, $\bar{h} = 0.7$, are shown in Fig. 4. The classical laminated theory (CLT) solutions are presented in Ref. 20, in which those solutions are reproduced by setting $\phi_\alpha = 0$ in the present theory. In Fig. 4, the △ data points indicate the solutions of higher-order theory (HOT) by Gu and Chattopadhyay.[13] The results of the present theory show good correlation with the CLT and HOT solutions.

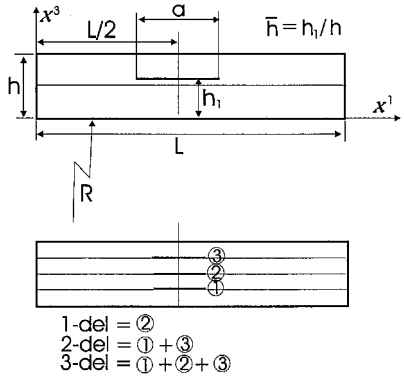

Fig. 3 Configuration of finite element model for the number of delaminations and their delamination thicknesses.

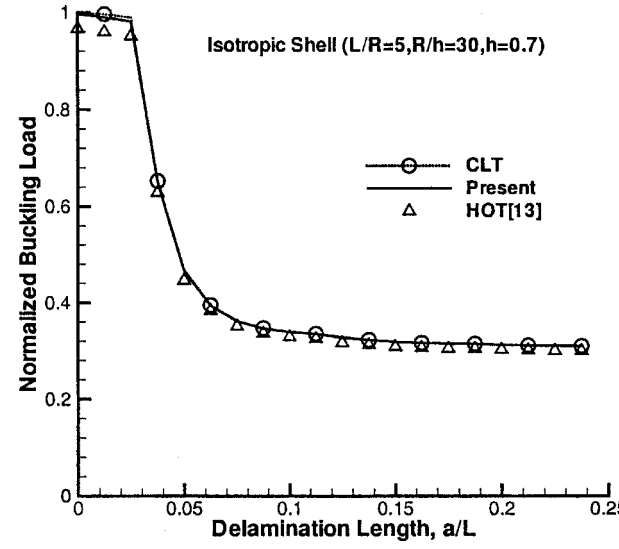

Fig. 4 Normalized buckling load for isotropic shell, $\bar{h} = 0.7$, for isotropic shell.

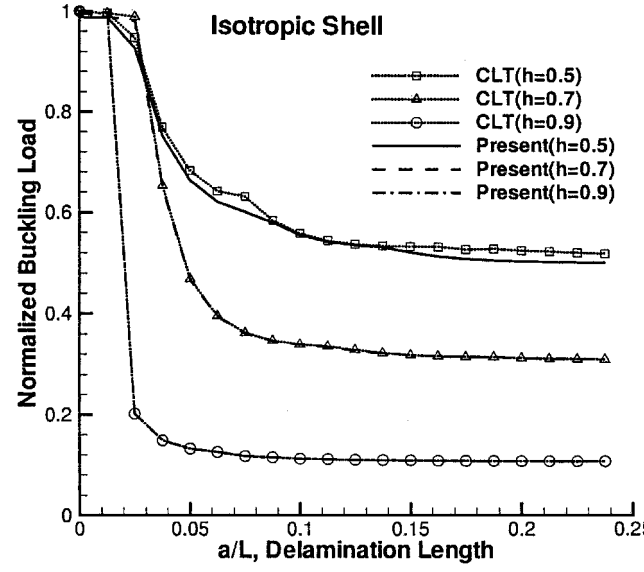

Fig. 5 Normalized buckling load with varying delamination thickness for isotropic shell.

The effect of delamination length on the critical loads of the shell, for different values of the delamination thickness is shown in Fig. 5. In this case, the normalized buckling loads are slightly lower than the CLT solutions. However, the buckling load patterns along the axial delamination length (a/L) are different from the CLT solutions at the delamination thickness, $\bar{h} = 0.5$. These different patterns indicate the change of the mode shapes. The symmetric and antisymmetric buckling loads of the present theory are presented in Fig. 6. In Fig. 6, the fundamental mode is varied from the antisymmetric mode to symmetric mode and from the symmetric mode to antisymmetric mode as the delamination length increases.

For comparison, we examine the same configuration solved by Sallam and Simitses.[20] The normalized buckling loads vs delamination length with a varying number of delaminations are shown on Fig. 7. This example demonstrates the effects of delamination length (a/L) and the number of delaminations on the buckling load

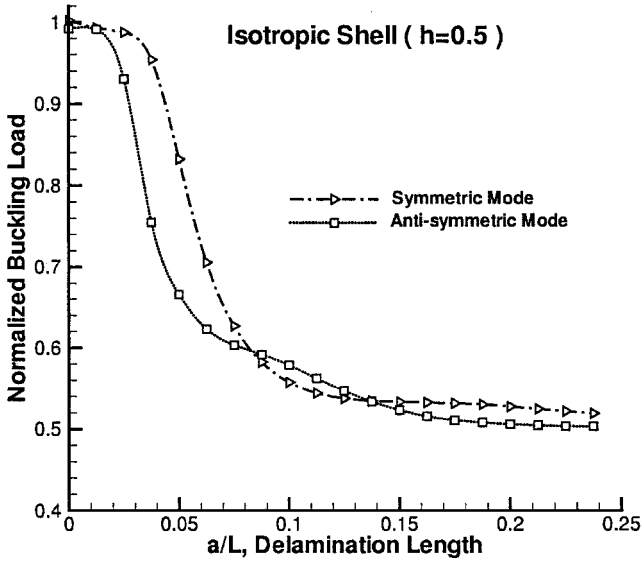

Fig. 6 Normalized buckling load for symmetric and antisymmetric mode, $\bar{h} = 0.5$, for isotropic shell.

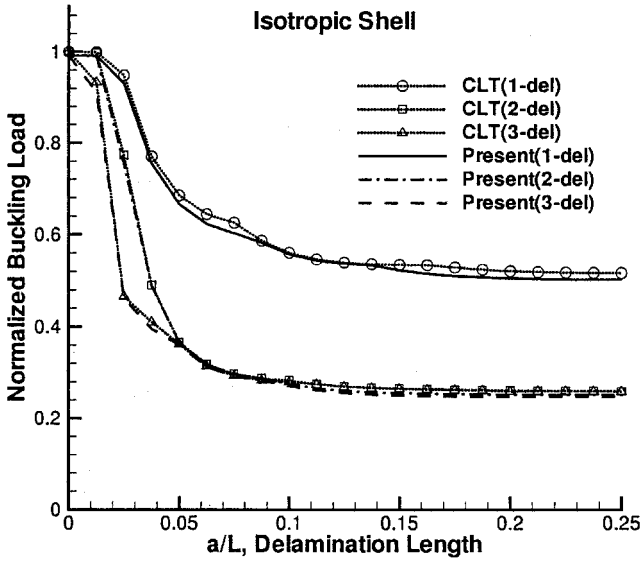

Fig. 7 Normalized buckling load with varying the number of delaminations for isotropic shell.

of laminated shells. Even in the case of multiple delaminations, the normalized buckling loads do not show significant deviations from the CLT solutions for $L/R = 5$. This observation agrees with that reported by Simitses and Anastasiadis.[21]

Figure 8 shows the axial and circumferential distributions of the buckling mode U_3 for $L/\hat{R} = 5$, $\hat{R}/h = 30$, and $\bar{h} = 0.75$. As shown in Fig. 8, the axial distribution of the buckling mode U_3 changes from a global to a local buckling mode as the length of delamination increase. Unlike the beam–plate case, the shell has a more complex mode shape for the circumferential direction.

B. Symmetric Composite Shell [0/90/90/0]

To compare the shear deformation effect, a clamped symmetric composite shell is considered. The dimensions of the shell are such that $L/\hat{R} = 5$ and $\hat{R}/h = 30$. The normalized buckling loads of the symmetric and antisymmetric modes are compared with those predicted by the CLT solutions in Fig. 9. The layup [0/90/90/0] in Fig. 9 indicates that there exists a delamination at the interface between two sublaminates (0/90) and (90/0), that is, the double slash denotes the delamination between layers. The buckling loads are lower than those of an isotropic shell of the same configuration ($\bar{h} = 0.5$). In addition, the change of the mode shape is observed as in the case of the isotropic shell.

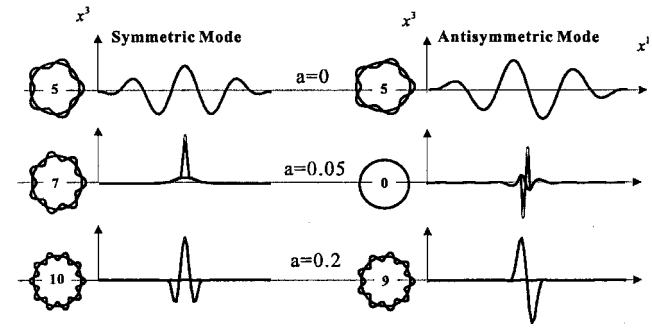

Fig. 8 Buckling mode shape for isotropic shell with $L/\hat{R} = 5$, $\hat{R}/h = 30$, and $\bar{h} = 0.75$.

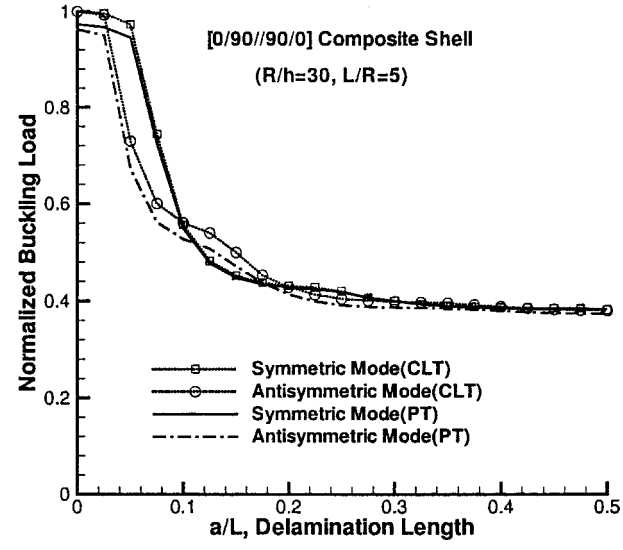

Fig. 9 Normalized buckling load for symmetric and antisymmetric mode, $\bar{h} = 0.5$, $L/\hat{R} = 5$, and [0/90//90/0].

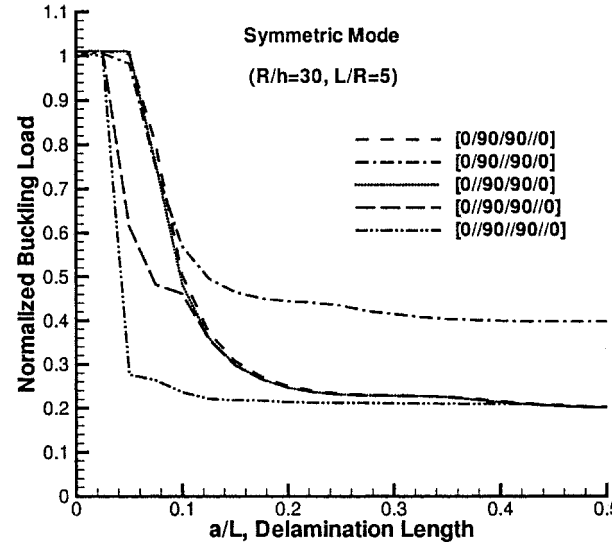

Fig. 10 Normalized buckling load with varying the number of delaminations for symmetric mode, $L/\hat{R} = 5$ and [0/90/90/0].

The buckling loads with a varying number of delaminations are shown in Fig. 10 for a symmetric mode. As shown in Fig. 10, for a single delamination, the buckling load indicates the lowest value when the delamination lies in the inner and outer interface. Note that the buckling load becomes highest when the delamination layer lies in the middle interface. In Fig. 11, the buckling loads for antisymmetric mode are presented. For the antisymmetric mode, the buckling load reaches the highest value when delamination lies in the inner interface with the delamination length $a/L < 0.15$.

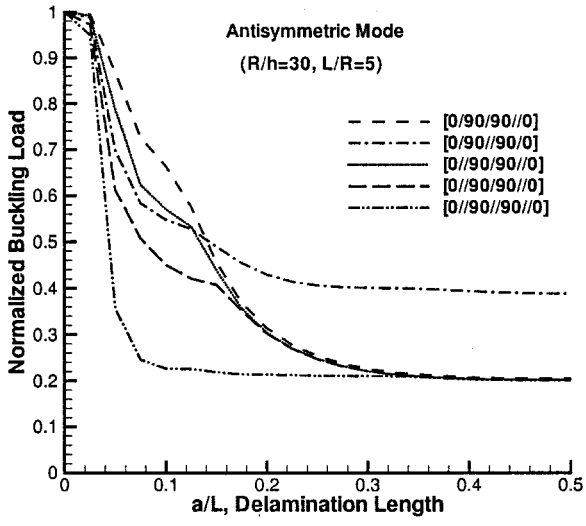

Fig. 11 Normalized buckling load with varying the number of delaminations for antisymmetric mode, $L/\hat{R} = 5$ and [0/90/90/0].

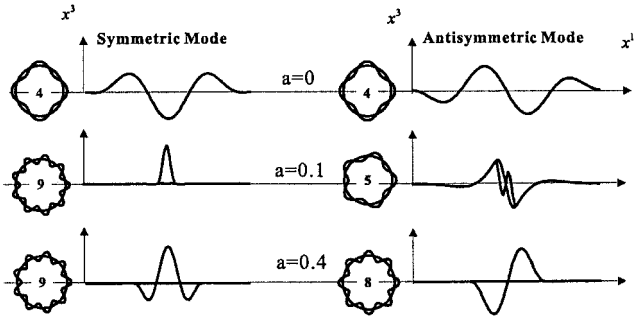

Fig. 12 Buckling mode shape for symmetric composite shell [0//90/90/0] with $L/\hat{R} = 5$ and $\hat{R}/h = 30$.

Figure 12 shows the axial and circumferential distributions of the buckling mode U_3 for the symmetric layup [0//90/90/0], $L/\hat{R} = 5$, and $\hat{R}/h = 30$. Note that the local buckling mode appears when the delamination length of the composite shell is longer than that of the isotropic shell. As shown, the changing pattern of buckling mode is similar to that of a delaminated isotropic shell.

C. Antisymmetric Cross-Ply Composite Shell [0/90/0/90]

To investigate the effect of the layup sequence, a clamped antisymmetric composite shell is considered. The dimensions of the shell are such that $L/\hat{R} = 5$ and $\hat{R}/h = 30$. A clamped antisymmetric shell containing one midsurface delamination is considered to compare the transverse shear effect. The normalized buckling loads of the symmetric and antisymmetric modes are compared with the CLT solutions in Fig. 13. For this case, the change of the mode is observed and is similar to that occurring in the case of symmetric composite shells with a similar configuration, but the sequence of the change of the mode is reversed, from the symmetric mode to the antisymmetric mode and from the antisymmetric mode to the symmetric mode.

The symmetric and antisymmetric buckling loads are presented in Figs. 14 and 15. For the symmetric mode of an antisymmetric composite shell with one delamination, the buckling load reaches the lowest value when the delamination lies at the inner interface.

D. Composite Shell [0//90/0/90] with Varying $L/\hat{R}$ and $\hat{R}/h$

The normalized buckling loads with variations of the radius to thickness ratio ($\hat{R}/h$) are shown in Figs. 16 and 17. In this example ($L/\hat{R} = 5$), the results of the present theory are compared with those of the CLT solutions. As shown in Fig. 16, for the symmetric mode, the transverse shear effect increases as the radius to thickness ratio ($\hat{R}/h$) decreases. However, for antisymmetric modes, the transverse shear effect is relatively smaller than for symmetric modes. For the

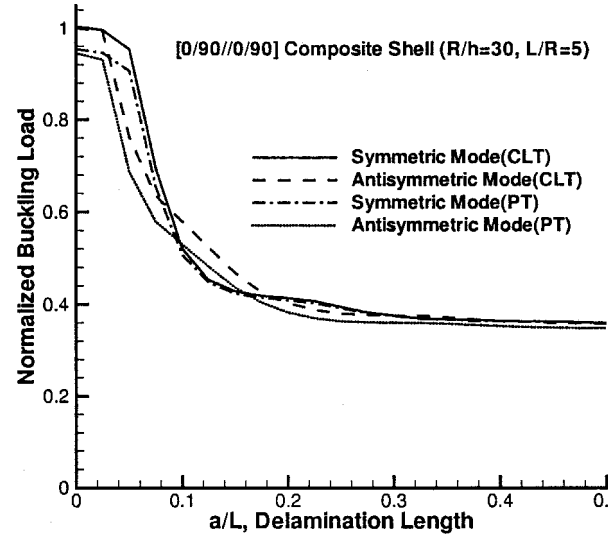

Fig. 13 Normalized buckling load for symmetric and antisymmetric mode, $\bar{h} = 0.5$, $L/\hat{R} = 5$, and [0/90/0/90].

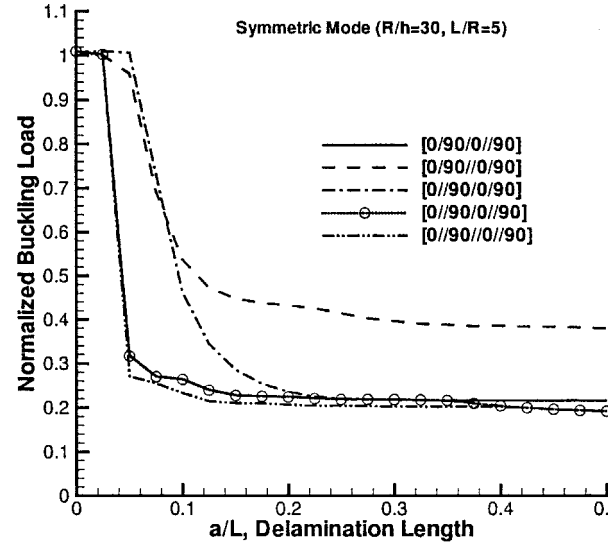

Fig. 14 Normalized buckling load with varying the number of delaminations for symmetric mode, $L/\hat{R} = 5$ and [0/90/0/90].

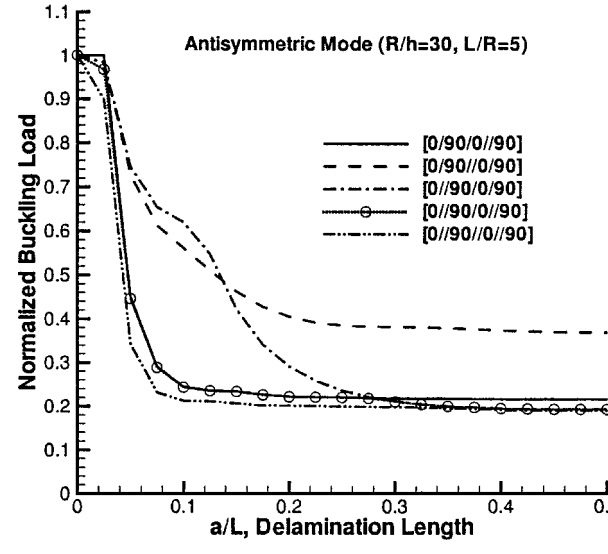

Fig. 15 Normalized buckling load with varying the number of delaminations for antisymmetric mode, $L/\hat{R} = 5$ and [0/90/0/90].

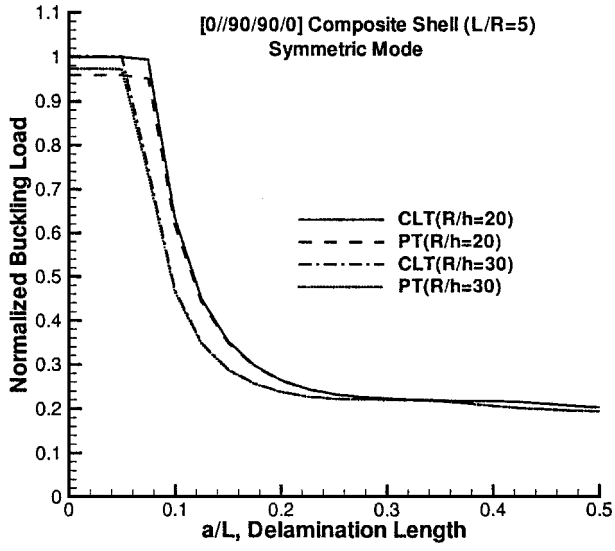

Fig. 16 Normalized buckling load with varying the $\hat{R}/h$ for symmetric mode, $L/\hat{R} = 5$ and [0//90/90/0].

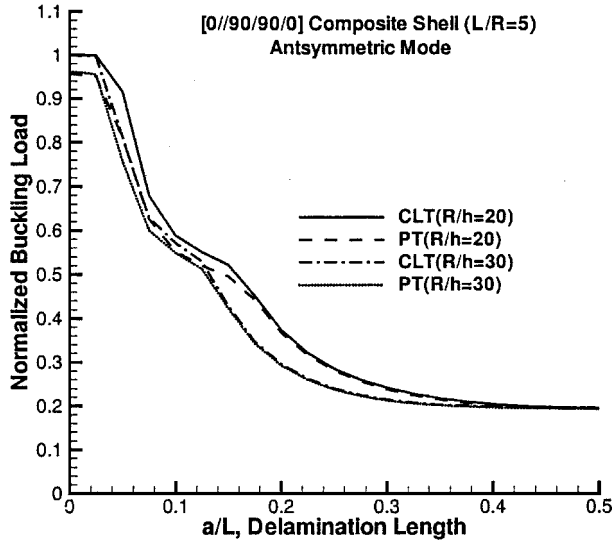

Fig. 17 Normalized buckling load with varying the $\hat{R}/h$ for antisymmetric mode, $L/\hat{R} = 5$ and [0//90/90/0].

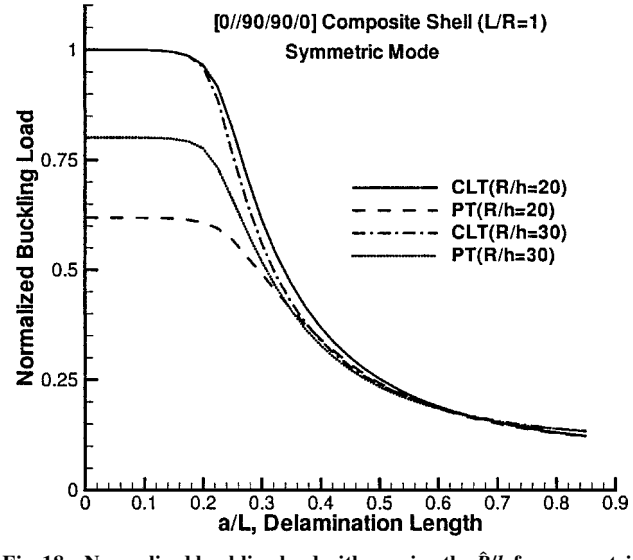

Fig. 18 Normalized buckling load with varying the $\hat{R}/h$ for symmetric mode, $L/\hat{R} = 1$ and [0//90/90/0].

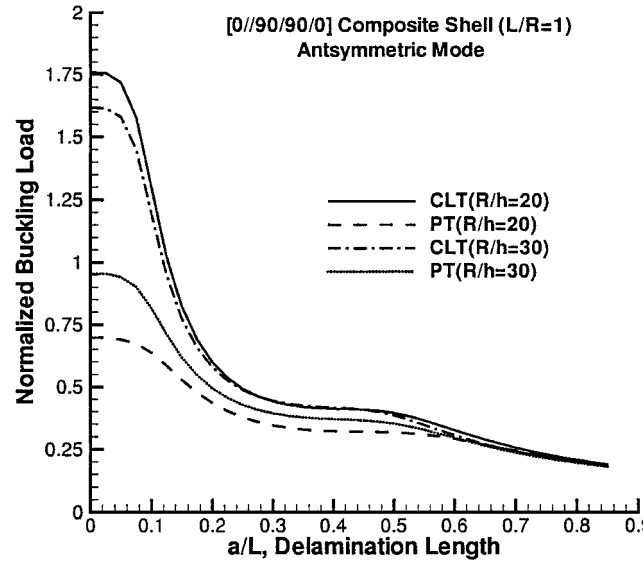

Fig. 19 Normalized buckling load with varying the $\hat{R}/h$ for antisymmetric mode, $L/\hat{R} = 1$ and [0//90/90/0].

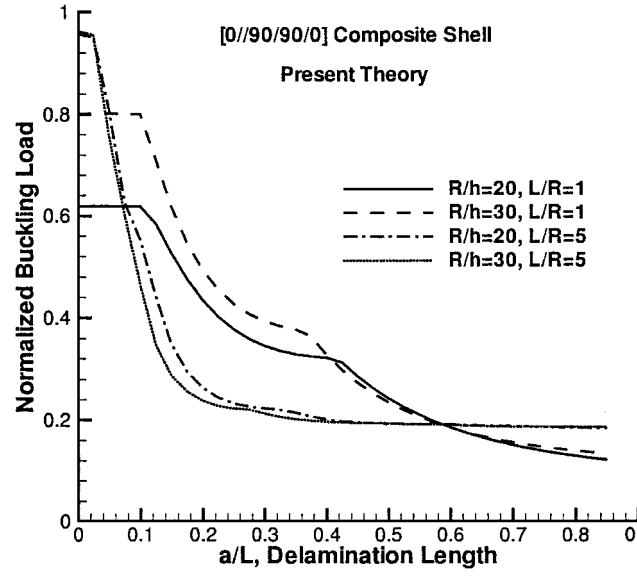

Fig. 20 Normalized buckling load with varying the $\hat{R}/h$ and $L/\hat{R}$, with [0//90/90/0].

length to radius ratio $L/\hat{R} = 1$, the symmetric and antisymmetric mode are presented in Figs. 18 and 19. The transverse shear effect is much more significant in the short cylinder ($L/\hat{R} = 1$) than that of the composite shell with $L/\hat{R} = 5$.

The normalized buckling loads with varying the radius to thickness ratio and the length to radius ratio are shown in Fig. 20, where the buckling loads are normalized with the corresponding CLT solutions. The transverse shear effect and the change of mode become significant when the length to radius ratio ($L/\hat{R}$) is changed. The effect of the radius to thickness ratio is relatively insignificant when comparing with that of the length to radius ratio.

VIII. Conclusions

A general tensor-based efficient higher-order shell theory for the general layup configurations is developed for laminated composites with multiple delaminations. Thus, a geometrically exact theory has been provided in the present study. The moderately large deflection in the von Kármán sense has been considered for the potential use in the postbuckling problem. It includes arbitrary oriented fiber direction and layer thickness. The shallow shell formulation is also obtained as a reduced form from that of the general formulation.

The present theory determines the number of degrees of freedom of the undelaminated zone independently of both the number of

layers and the number of delaminations. In the delaminated zone, the minimal number of degrees of freedom is still retained. Thus, this theory can be applied to laminated shells of arbitrary geometry with many layers and multiple delaminations.

The validity and efficiency of the present theory have been demonstrated in linear bucking problems through semi-analytical finite element analysis. The finite element analysis procedures can be directly extended to the problems of postbuckling behavior of shells with multiple delaminations, which is now under progress.

Acknowledgments

This research was supported by the Micro Thermal System Research Center through the Korea Science and Engineering Foundation.

References

[1]Noor, A. K., and Burton, W. S., "Assessment of Computational Models for Multilayered Composite Plates and Shells," *Applied Mechanics Reviews*, Vol. 45, No. 4, 1990, pp. 67–97.

[2]Reddy, J. N., and Robbins, D. H., Jr., "Theories and Computational Models for Composite Laminates," *Applied Mechanics Reviews*, Vol. 47, No. 1, 1994, pp. 147–169.

[3]Whitney, J. M., and Sun, C. T., "A Refined Theory for Laminated Anisotropic Cylindrical Shells," *Journal of Applied Mechanics*, Vol. 41, No. 2, 1974, pp. 471–476.

[4]Reddy, J. N., and Liu, C. F., "A Higher-Order Shear Deformation Theory of Laminated Elastic Shells," *International Journal of Engineering Science*, Vol. 23, No. 3, 1985, pp. 319–330.

[5]Barbero, E. J., and Reddy, J. N., "General Two-Dimensional Theory of Laminated Cylindrical Shells," *AIAA Journal*, Vol. 28, No. 3, 1990, pp. 544–553.

[6]Di Sciuva, M., "An Improved Shear-Deformation Theory for Moderately Thick Multilayered Anisotropic Shells and Plates," *Journal of Applied Mechanics*, Vol. 54, No. 3, 1987, pp. 589–596.

[7]He, L.-H., "A Linear Theory of Laminated Shells Accounting for Continuity of Displacements and Transverse Shear Stresses at Layer Interfaces," *International Journal of Solids and Structures*, Vol. 31, No. 5, 1994, pp. 613–627.

[8]Ossadzow, C., Touratier, M., and Muller, P., "Deep Doubly Curved Multilayered Shell Theory," *AIAA Journal*, Vol. 37, No. 1, 1999, pp. 100–109.

[9]Cheng, Z.-Q., Kennedy, D., and Williams, F. W., "Effect of Interfacial Imperfection on Buckling and Bending Behavior of Composite Laminates," *AIAA Journal*, Vol. 34, No. 12, 1996, pp. 2590–2595.

[10]Cheng, Z.-Q., and Kitipornchai, S., "Nonlinear Theory for Composite Laminated Shells with Interfacial Damage," *Journal of Applied Mechanics*, Vol. 65, No. 3, 1998, pp. 711–718.

[11]Di Sciuva, M., "Geometrically Nonlinear Theory of Multilayered Plates with Interlayer Slips," *AIAA Journal*, Vol. 35, No. 11, 1997, pp. 1753–1759.

[12]Cho, M., and Kim, J.-S., "Buckling Analysis for Laminated Plates with Multiple Delaminations," *Journal of Applied Mechanics* (to be published).

[13]Gu, H., and Chattopadhyay, A., "Delamination Buckling and Postbuckling of Composite Cylindrical Shells," *AIAA Journal*, Vol. 34, No. 6, 1996, pp. 1279–1286.

[14]Naghdi, P. M., "Foundation of Elastic Shell Theory," *Progress of Solids Mechanics*, edited by I. N. Sneddon and R. Hill, Vol. 4, North-Holland, Amsterdam, 1963, Chap. 1.

[15]Librescu, L., *Elastostatics and Kinetics of Anisotropic and Heterogeneous Shell-Type Structures*, Noordhoff International, Leyden, The Netherlands, 1975.

[16]Green, A. E., and Zerna, W., *Theoretical Elasticity*, Clarendon, Oxford, 1954, pp. 1–39.

[17]Librescu, L., and Schmidt, R., "Substantiation of a Shear-Deformable Theory of Anisotropic Composite Laminated Shells Accounting for the Interlaminar Continuity Conditions," *International Journal of Engineering Science*, Vol. 29, No. 6, 1991, pp. 669–684.

[18]Schmidt, R., and Librescu, L., "A General Theory of Geometrically Imperfect Laminates Composite Shells Featuring Damages Bonding Interfaces Laminated Shells Featuring Interlaminar Bonding Imperfections," *Quarterly Journal of Applied Mathematics*, Vol. 52, No. 4, 1999, pp. 565–583.

[19]Librescu, L., and Schmidt, R., "A General Linear Theory of Laminated Shells Featuring Interlaminar Bonding Imperfections," *International Journal of Solids and Structures*, Vol. 38, No. 19, 2001, pp. 3355–3375.

[20]Sallam, S., and Simitses, G. J., "Delamination Bucking of Cylindrical Shells Under Axial Compression," *Composite Structures*, Vol. 7, No. 1, 1987, pp. 83–101.

[21]Simitses, G. J., and Anastasiadis, J. S., "Shear Deformable Theories for Cylindrical Laminates Equilibrium and Buckling with Applications," *AIAA Journal*, Vol. 30, No. 3, 1992, pp. 826–834.

A. Chattopadhyay
Associate Editor